Proc. Natl. Acad. Sci. USA
Vol. 94, pp. 14683–14688, December 1997
Medical Sciences

The anticoagulant activation of antithrombin by heparin

(serpins/thrombosis/heparans/conformational mobility)

LEI JIN*, JAN PIETER ABRAHAMS†‡, RICHARD SKINNER*, MAURICE PETITOU§, ROBERT N. PIKE*, AND ROBIN W. CARRELL*

*Department of Haematology, University of Cambridge, and †Laboratory of Molecular Biology, Medical Research Council Centre, Hills Road, Cambridge CB2 2QH, United Kingdom; and §Haemobiology Research Department, Sanofi Recherche, 195 Route d'Espagne, B.P.1169-31036 Toulouse Cedex, France

Communicated by Max F. Perutz, Medical Research Council, Cambridge, United Kingdom, October 20, 1997 (received for review May 22, 1997)

ABSTRACT **Antithrombin, a plasma serpin, is relatively inactive as an inhibitor of the coagulation proteases until it binds to the heparan side chains that line the microvasculature. The binding specifically occurs to a core pentasaccharide present both in the heparans and in their therapeutic derivative heparin. The accompanying conformational change of antithrombin is revealed in a 2.9-Å structure of a dimer of latent and active antithrombins, each in complex with the high-affinity pentasaccharide. Inhibitory activation results from a shift in the main sheet of the molecule from a partially six-stranded to a five-stranded form, with extrusion of the reactive center loop to give a more exposed orientation. There is a tilting and elongation of helix D with the formation of a 2-turn helix P between the C and D helices. Concomitant conformational changes at the heparin binding site explain both the initial tight binding of antithrombin to the heparans and the subsequent release of the antithrombin–protease complex into the circulation. The pentasaccharide binds by hydrogen bonding of its sulfates and carboxylates to Arg-129 and Lys-125 in the D-helix, to Arg-46 and Arg-47 in the A-helix, to Lys-114 and Glu-113 in the P-helix, and to Lys-11 and Arg-13 in a cleft formed by the amino terminus. This clear definition of the binding site will provide a structural basis for developing heparin analogues that are more specific toward their intended target antithrombin and therefore less likely to exhibit side effects.**

Heparin, a sulfated polysaccharide, is second only to insulin as a natural therapeutic agent and is the initial-choice anticoagulant in the treatment and prevention of thromboembolic disease. It functions in life as a component of the heparans that line the inner walls of the microvascular system (1), but heparin as a drug is a heterogeneous animal extract administered by injection to circulate in the bloodstream. Both heparin and the natural heparans contain a specific pentasaccharide fragment (2, 3) that binds and activates the plasma proteinase inhibitor antithrombin.

In nature, this binding to heparans substantially localizes the function of antithrombin to inhibition of the serine proteases of the coagulation cascade within the bloodstream, allowing their coagulant activity in damaged tissue outside the vascular system. The heparans and the longer-chain heparins (4) activate the inhibition of thrombin by antithrombin by bringing them into close apposition, but there is also a direct activation of inhibition due to an overall conformational change (5) induced by the binding to the core pentasaccharide present in both heparin and heparans. This pentasaccharide-induced change alters the conformation of the reactive site loop of antithrombin (6, 7) and gives a 300-fold increase in inhibitory activity against the key coagulation protease factor Xa. Linked to this is a change in affinity at the heparin binding site (see Fig. 1), and as antithrombin contacts the pentasaccharide, it moves from an initial low-affinity to high-affinity heparin binding. It then reverts to low-affinity binding on formation of the complex with the protease, thus allowing the release of the antithrombin–protease complex from the heparans into the circulation.

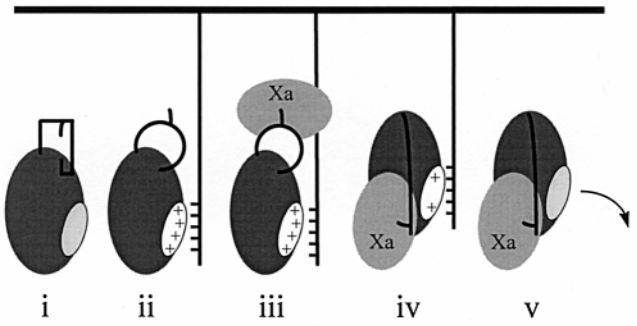

FIG. 1. Schematic: i, circulating antithrombin; ii, contacts endothelial heparans with induction of high-affinity binding and reactive site loop exposure; iii–iv, complexes with factor Xa followed by loop cleavage and insertion with diminished heparin affinity; and v, the complex is released into the circulation for catabolism by the liver.

The molecular mobility necessary for such linked conformational changes is inherent to antithrombin (8), a member of the serpin family of serine protease inhibitors (9). The serpins have a mobile reactive site loop that is initially exposed as a substrate for cognate proteases. On cleavage by the protease the loop becomes inserted as a sixth strand in the central β-sheet (the A-sheet) of the molecule (10). In this way the protease is believed to be irreversibly trapped as a reaction intermediate covalently bound to the serpin (11). The change from a five-stranded to a six-stranded A-sheet (12) is accompanied by a profound conformational change that occurs not only in the cleaved form but also in the nonphysiological latent conformation in which the intact reactive loop is inserted into the A-sheet. The structures of both inhibitory and latent antithrombin (referred to as I- and L-antithrombin, respectively) have been well studied (13–15) as the two forms readily cocrystallize as a dimer. Here, we describe a related crystal form in which both antithrombin molecules are in complex with the core pentasaccharide fragment of heparin (16) modified by an additional sulfate (17) to give higher affinity binding (K_d 0.4 nM vs. 50 nM).

The publication costs of this article were defrayed in part by page charge payment. This article must therefore be hereby marked "*advertisement*" in accordance with 18 U.S.C. §1734 solely to indicate this fact.

Data deposition: The atomic coordinates reported in this paper have been deposited in the Protein Data Bank, Biology Department, Brookhaven National Laboratory, Upton, NY 11973 (reference 1ZX) and will be released after 1 year.

‡To whom reprint requests should be addressed at: Gorlaeus Laboratories, P.O. Box 9502, 2300 RA Leiden, The Netherlands. e-mail: abrahams@chem.leidenuniv.nl.

MATERIALS AND METHODS

Crystallization. I-antithrombin was purified from human plasma (14) and stored in 20 mM Tris·HCl, pH 8.0. L-antithrombin was prepared (14) by incubating I-antithrombin (at 1 mg/ml) at 60°C for 15 hr in 20 mM Tris/0.25 M sodium citrate, pH 7.4. It was purified by heparin-Sepharose (eluted at 0.4 M NaCl, whereas normal antithrombin is eluted at 0.8 M NaCl) and ion-exchange chromatography and then concentrated in 20 mM Tris·HCl, pH 8.0. The synthetic (17) high-affinity pentasaccharide (compound 83 in ref. 16) varied from the natural pentasaccharide in having an extra sulfate in saccharide H (Fig. 2*c*). Heterodimeric antithrombin crystals grew within 1 week at 18–20°C after a 1:1 stoichiometric mixing of 2 μl of active antithrombin (40 mg/ml), 6.6 μl of L-antithrombin (12.2 mg/ml), with a slight molar excess of pentasaccharide (1.4 μl of 4 mg/ml in deionized water), and 10 μl of 30% (wt/vol) PEG4000 in 0.05% NaN_3/0.1 M sodium cacodylate, pH 7.0.

Data Collection. Diffraction data were collected on an MAR Research image plate by using synchrotron radiation (wavelength 0.87 Å, station 9.6 at Daresbury, U.K.) from a frozen crystal (space group P21, unit cell: a = 70.44 Å, b = 86.97 Å, c = 97.22 Å, β = 108.88°) at 100 K. Immediately before freezing, the crystal was immersed in cryoprotectant [25% (vol/vol) 2-methyl-2,4-pentanediol/18% (wt/vol) PEG4000/40 mM sodium cacodylate, pH 7.0) for 4 sec and then mounted in the N_2 stream. The data were integrated by using MOSFLM (18) and processed with programs from the CCP4 (19) suite (see Table 1).

Structure Determination. The structure was solved by molecular replacement using AMoRe (20) with the 2.6-Å antithrombin structure as search model (15). Manual rebuilding was carried out with the program O (21) using σ_A-weighted $2F_o - F_c$ and $F_o - F_c$ electron density maps. Models were refined using the TNT (22) suite and XPLOR (23) with grouped temperature factors. Two pentasaccharide moieties, bound to I- and L-antithrombin, were built into clear difference density once the free R-factor had dropped below 35%. This model was used to remove the anisotropy of the overall temperature factor of the crystallographic data. The final model has a free R-factor of 28.8% and excellent stereochemistry (see Table 1) (24). Exposed peptide loops in the body of the molecule, including the critical hD-s2A (137–139) and reactive center (378–386) loops, had high temperature factors, but the electron density was continuous and allowed unambiguous tracing of the chain. Figures were produced with MOLSCRIPT (25) and BOBSCRIPT (R. Esnouf).

Treatment of Antithrombin with Peptidylarginine Deiminase. Antithrombin Glasgow (P_1 Arg → His) was a gift from M. C. Owen (26). Antithrombin (10 μM) was incubated with peptidylarginine deiminase (Panvera, Madison, WI) at a molar ratio of 50:1 (inhibitor:enzyme) in 100 mM Tris·HCl/5 mM $CaCl_2$, pH 7.4, for 16 hr at 37°C in the presence or absence of heparin pentasaccharide (50 μM). The reaction was stopped with 50 mM EDTA and the products were analyzed on native 7.5% polyacrylamide gel electrophoresis.

RESULTS AND DISCUSSION

The crystal packing of the I- and L-antithrombin dimers, in complex with the pentasaccharide (Fig. 2*a*), is similar to that of the crystal forms in the absence of the heparin fragment (13–15) despite a marked difference in the unit cell dimensions. The electron density of the pentasaccharide is well defined in both molecules (Fig. 2 *a* and *b*), and the relations of its negatively charged carboxylate and sulfate groups to arginyl and lysyl side chains on antithrombin (Fig. 2*c*) are clearly evident. As predicted (9, 27), binding occurs to the upper half of the D-helix (Lys-125, Arg-129) and the base of the A-helix (Arg-47 and Arg-46 and also the main-chain amide of Asn-45). On the other side of the pentasaccharide, there is binding to the amino terminus of antithrombin through the side chains of Lys-11 and Arg-13 as well as the main-chain amide of Arg-13. Further direct hydrogen bonds to the pentasaccharide (28) are made by the side chain of Lys-114 and the main-chain amides of Glu-113 and Lys-114, which are each brought into H-bonding proximation as a consequence of an induced new helix (named P for the pentasaccharide) between the C and D helices.

Table 1. Summary of crystallographic data

Data	Value
Resolution range, Å	30–2.9
Total number of reflections	24,096
Completeness, %	94.2
R_{merge},* %	12.4
Rejected outliers,† %	0.2
Mean $\langle F/\sigma \rangle$	5.2
Multiplicity	2.5
R-factor,‡ %	20.3
Free R-factor,§ %	28.7
Number of atoms per asymmetric unit	
Protein	6,643
Carbohydrate	42
Pentasaccharide	200
rmsd bond length,¶ Å	0.005
rmsd bond angle,¶ °	1.0
Main-chain torsion angles‖¶	84.3% (preferred) 14.2% (allowed) 1.3% (generously allowed)

Average temperature factors, Å^3	Mean	SD
L-molecule	32.46	21.97
L-molecule pentasaccharide**	35.84	11.18
I-molecule	38.58	22.49
I-molecule pentasaccharide	48.14	10.15

*R_{merge}** = $\Sigma\Sigma_i|I(h) - I(h)_i|/\Sigma\Sigma_i|I(h)_i|$, where $I(h)$ is the measured mean intensity after rejections.

†Reflections observed more than twice, and with intensities differing by more than 3.5 $\sigma(I)$ from the weighted mean were rejected. The fraction of the total number of measured reflections is given.

‡The crystallographic R-factor of data between 6.0 and 2.9 Å after the final round of refinement.

§The free R-factor of 851 randomly selected reflections (6.0–2.9 Å) after final round of refinement.

¶From PROCHECK (24) (rmsd, root mean square deviation from ideal values).

‖The generously allowed and disallowed ϕ–ψ torsion angles are found in poorly ordered loops.

**The L-molecule pentasaccharide has a lower B-factor due to an additional crystal contact.

A comparison of the crystal structures of I- and L- antithrombins both before (15) and after complexing with the pentasaccharide reveals the detailed molecular mechanisms for the sequence of changes shown diagrammatically in Fig. 1. The initial changes that follow binding of the pentasaccharide (Fig. 1, i–ii) are evident on comparing the uncomplexed and complexed I-molecules, which show striking conformational rearrangements most notably around the heparin binding site. Of all C^α atoms, 60% can be aligned with an rms distance of 0.5 Å, when deviations larger that 1 Å are discarded; the main differences are found in the stretches 5–48, 108–199, 203–215, 218–223, 324–329, 353–362, 379–386, and 414–419. The first contribution to these changes can be explained by the necessity to accommodate the pentasaccharide. The less well ordered amino-terminal residues 12–16 shift sideways, widening the cleft where the pentasaccharide binds. The N terminus of the

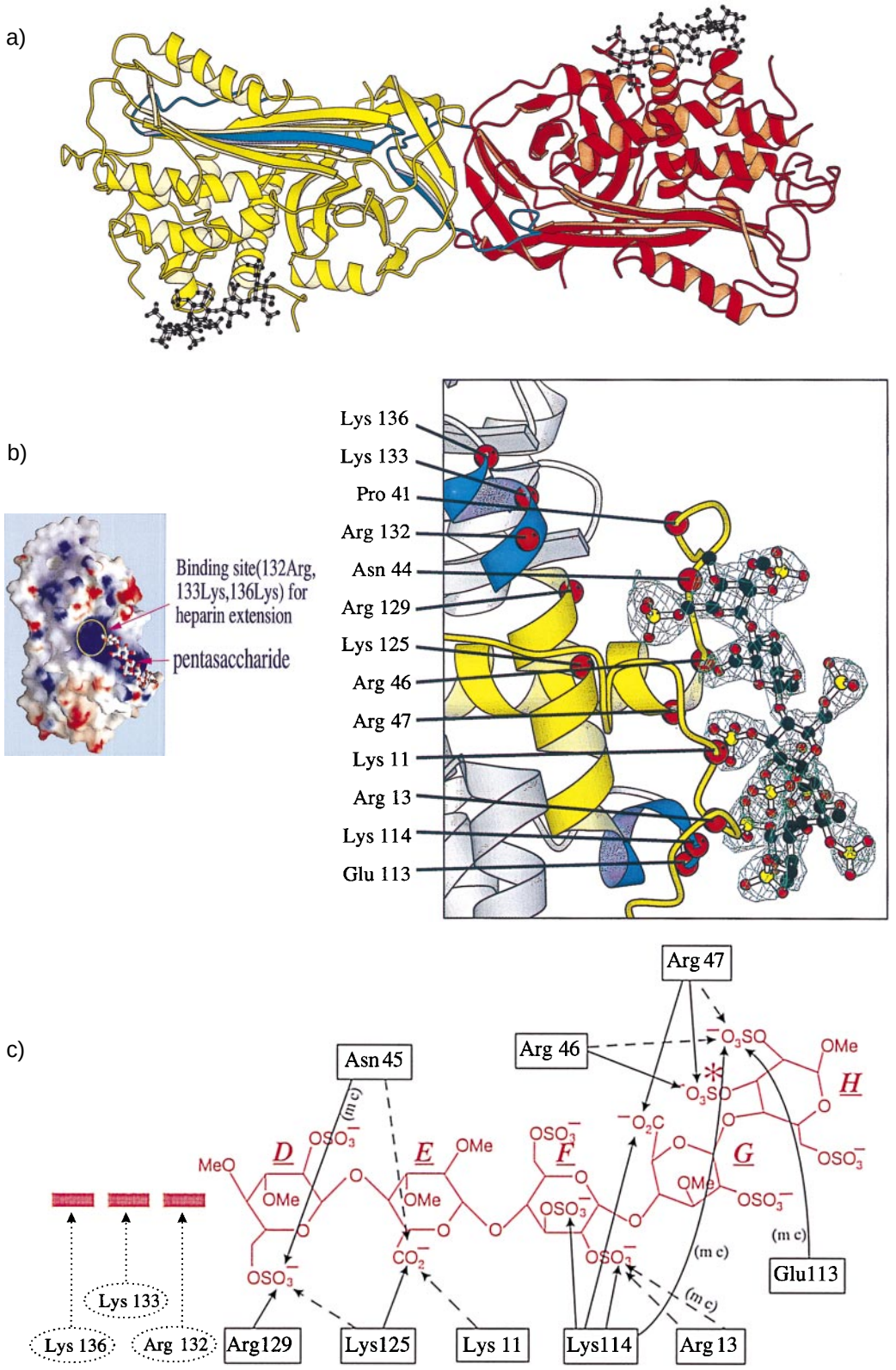

FIG. 2. (*a*) Dimer of L-antithrombin (yellow) and I-antithrombin (red) each complexed with the pentasaccharide (black). The reactive site loop of each molecule is in blue, the loop being fully inserted in the A β-sheet in L-antithrombin with the reactive loop of the I-antithrombin replacing the vacated strand site s1C in the L-molecule through its P_3–P_8 residues (amino-terminal to the P_1 reactive center). (*b*) (*Left*) Electrostatic surface potential map of antithrombin (red, negative potential; blue, positive potential) with the pentasaccharide outline and showing its extension region including 132-Arg, 133-Lys, and 136-Lys. (*Right*) A σ_A-weighted difference map, calculated after omitting the pentasaccharide, is displayed at a contour level of 3σ within volume 4 Å around the omitted atoms. Superimposed on the omitmap are the atoms of the pentasaccharide DEFGH (D above) and a ribbon representation of I-antithrombin. The binding site is in yellow and also includes the P-helix, the lower of the two induced helical segments, in blue. (*c*) Hydrogen bonding to pentasaccharide DEFGH. Likely bonds in full lines, possible bonds in interrupted lines, (mc) indicates main-chain bonding. Arg-132, Lys-133, and Lys-136 are beyond hydrogen bonding distance from the pentasaccharide but could interact with extended oligosaccharides. The extra sulfate present in the high affinity pentasaccharide (16) is asterisked in saccharide H.

A-helix rearranges, allowing the primary amines of Arg-46 and Arg-47 to move by 17 and 8 Å, respectively, to hydrogen bond with the sulfate residues of the pentasaccharide, whereas residues 44 and 45 make way for the cofactor. The D-helix tilts by some 10°, whereas at its amino terminus, residues 113–118 coil to form the two-turn P-helix at right angles with the D-helix. At the carboxyl terminus, the D-helix is extended by one-and-a-half turns, moving Arg-132, Lys-133, and Lys-136 toward the pentasaccharide binding site. These residues do not come within hydrogen bonding distance of the pentasaccharide. However, they would be able to interact with additional saccharide units of full-length heparin.

The other main contributor to the differences between the complexed and uncomplexed I-molecules is the movements involved in the activation of antithrombin toward factor Xa (Fig. 1, ii). The closing of the A-sheet with an accompanying expulsion of the partially inserted residues P_{14} and P_{15} of the reactive site loop (Fig. 3) occurs by an allosteric mechanism as it is more than 30 Å distant from the pentasaccharide. The closure of the A-sheet is at least in part a response, as predicted (29), to the one-and-a-half turn extension of the D-helix. There is no direct interaction between the pentasaccharide and the extra turns of the helix, and the extension is probably driven by the favorable effect of the neutralization of the charges of Lys-125 and Arg-129 in the turns preceding the elongation.

The comparison of the I- and L- molecules indicate the changes that follow the formation of the complex with factor Xa by the pentasaccharide-activated antithrombin, as represented in Fig. 1, iii–v. The main conformational change in going from I- to L- antithrombin (15) is the insertion of the reactive loop as a sixth strand into the A-sheet (Fig. 2*a*). Electron density of residues 391–404 of the latent loop are visible in the complex with the pentasaccharide, confirming that the loop is not cleaved during crystallization. The presence of the pentasaccharide induces the same conformation around its binding site in L-antithrombin as in I-antithrombin, with the notable exception of the carboxyl terminus of the D-helix, which is not extended in L-antithrombin but instead is present as a poorly ordered loop. As a result, Arg-132 and Lys-133 no longer adopt a conformation in which they would be able to interact with the longer polysaccharide heparin, unlike in pentasaccharide-activated I-antithrombin. This difference between I- and L-antithrombin is caused by the lateral expansion of the A-sheet, which results from the insertion of the reactive loop, thus taking up the space otherwise occupied by the extended D-helix. This observation explains why cleaved antithrombin (30), which is conformationally closely related to L-antithrombin and also to that of the assumed final complex (Fig. 1, iv), more readily dissociates from full-length heparin than I-antithrombin.

Surprisingly, the structural interaction of the pentasaccharide with I-antithrombin is otherwise identical with that of L-antithrombin, including the conformation of the pentasaccharide itself. We conclude therefore that the decreased affinity for the pentasaccharide of the six-stranded forms of antithrombin must at least in part be caused by a different initial association rate. This is in keeping with an earlier crystallographic study (15) of a similar heterodimer of antithrombin, in the absence of the pentasaccharide, showing a shielding of the heparin binding site in L-antithrombin but not in I-antithrombin.

The studies described here demonstrate how evolution has adapted the inherent molecular mobility of antithrombin to meet a specialized physiological need. As opposed to other serpins, antithrombin circulates with its reactive center arginine obscured (Fig. 3) and hence less vulnerable to incidental cleavage (31). This is achieved by holding the reactive site loop partially inserted into the A-sheet of the molecule until the loop is released when antithrombin binds to the pentasaccharide core of the heparans. Thus, the linkage of the change of conformation at the pentasaccharide binding site with the exposure of the reactive loop ensures that full activation of antithrombin does not occur until it is bound to the walls of the microvasculature.

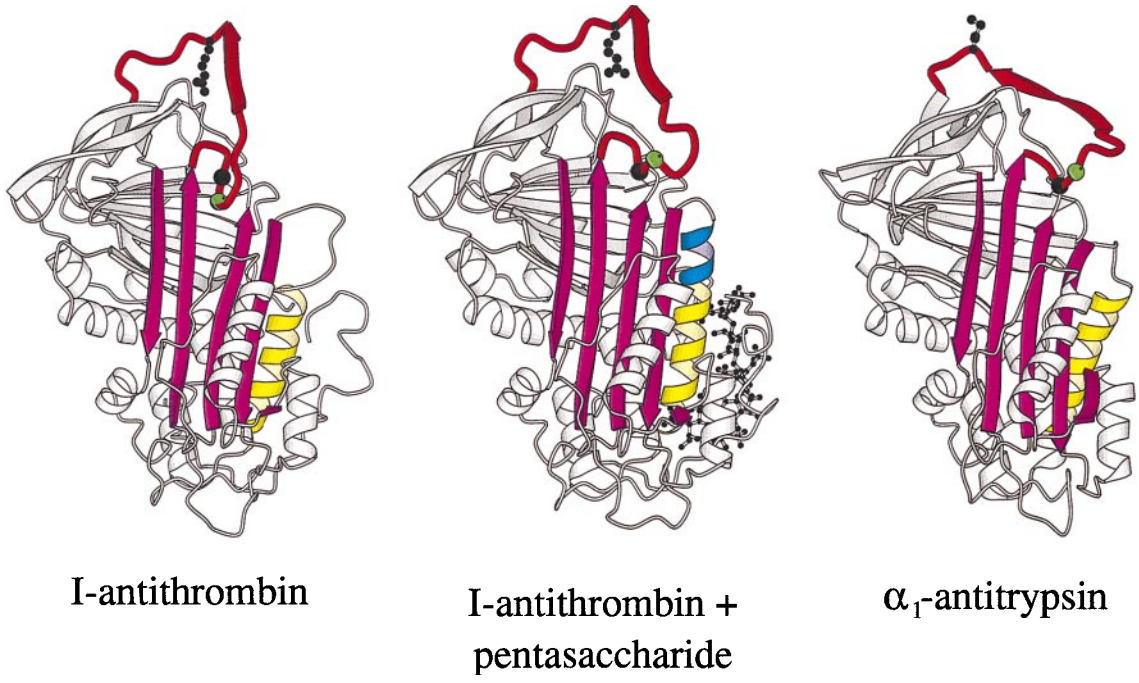

FIG. 3. Ribbon diagrams of (from left) I-antithrombin (15), pentasaccharide-complexed I-antithrombin, and α_1-antitrypsin (32). The pentasaccharide activation of I-antithrombin is seen to involve a closing of the A-sheet (magenta), an extension (blue) of helix D (yellow), and an expulsion of residues P_{14} (green sphere) and P_{15} (black sphere) of the reactive site loop (red). The reactive loop of both antithrombin molecules is constrained by the dimer contact (see Fig. 2*a*) of the β-pleated P_3–P_8 (ribboned arrow). An indication of the likely free conformation, with exposure of the P_1 reactive center (shown as a ball–stick model), is provided by the optimal inhibitory conformation of the reactive loop present in α_1-antitrypsin (32).

The release of the reactive loop from the A-sheet leaves it free to take up an optimal inhibitory conformation, though in the crystal structures this is limited by the dimer contact of residues P_3–P_8 of the loop (P_n–P_n are numbered amino-terminally with respect to the P_1 reactive center) (Fig. 2*a*). A model of the likely unrestrained reactive-site conformation is provided by the recent crystal structure of α_1-antitrypsin (32), with a reactive loop in the exposed canonical form that matches the complementary conformation of the active site of the serine proteases. In this conformation, the side chain of the reactive center P_1 residue is fully exposed (Fig. 3), and we believe that the full activation of antithrombin will also involve movement of the side chain of the P_1 arginine from its internal to a similar external orientation. Direct evidence for such a reorientation comes from recent studies (33) in which the accessibility of the side chain of the P_1 Arg was probed with peptidyl deiminase (34). These studies show that the P_1 side chain is protected in the absence of the pentasaccharide but becomes vulnerable to attack in the presence of the pentasaccharide (Fig. 4). Furthermore, as predicted by this mechanism, the deimination of the P_1 Arg, with consequent loss of its hydrogen bonding to the body of the molecule, results in a reversion of antithrombin to the higher heparin-affinity conformation (33).

Previous predictions as to the heparin binding site (9, 27, 28, 35), and to the movement (6), extrusion (29), and activation (5, 7, 8, 32, 36) of the reactive loop of antithrombin, are in general agreement with the structural changes observed here. The series of structures we have described connect the changes with each other and also show the detailed molecular interactions involved. An example of the value of this detail is provided by the natural mutations of antithrombin that produce familial thromboembolic disease. We could previously readily explain (14) the consequences of the replacement of basic residues at the binding site, for instance of Arg-47 or Arg-129. Now, however, there is also a satisfying explanation for the thromboembolic disease that results from the replacement of Pro-41, which is seen to form a critical turn at the point of entry of saccharides DE to the binding site (Fig. 2*b*). Similarly, the thrombotic consequences of the substitutions of other residues by prolines at 116 and 118 now become clear as a predictable disruption of the new P-helix (113–118) and hence of the binding of Lys-114 and Glu-113 to the pentasaccharide.

The detailed binding interactions of antithrombin with the pentasaccharide also agree with the systematic studies (16) of the binding of some 90 different modifications and analogues of the heparin pentasaccharide. These studies have led to the identification of modified pentasaccharides of increased activity, including the pentasaccharide used here, which has an extra sulfate group on saccharide H. The new knowledge of the detailed binding interactions with antithrombin gives the potential to design further modifications of the core pentasaccharide, as indicated in Fig. 2*b*, to give increased specificity of binding and activation. There are good reasons for doing this, as current therapy with heparin is limited by its heterogeneity, with some of the oligosaccharide binding to blood platelets causing their aggregation by immune mechanisms to give the distressing disorder thrombotic thrombocytopenia (37). In the longer term, the new structures also open the prospect (38) of the design of nonsaccharide mimetics, which, unlike heparin, could be administered orally.

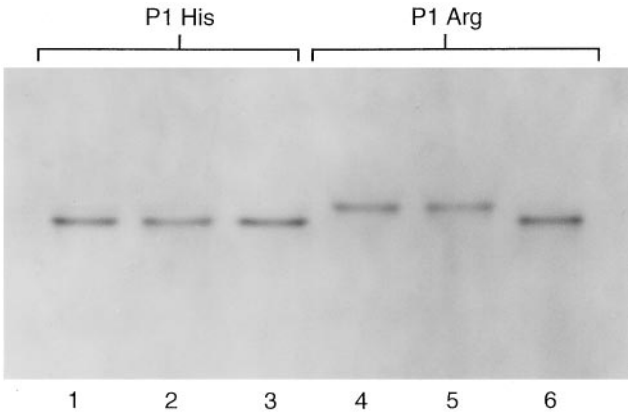

FIG. 4. Exposure of reactive center arginine by pentasaccharide. Native PAGE at pH 8.0 of a mutant (P_1 His) antithrombin (26) in lanes 1–3, and of normal (P_1 Arg) antithrombin in lanes 4–6, is shown. In lanes 2 and 5, the antithrombins have been incubated with deiminase; in lanes 3 and 6, incubation with deiminase has been carried out in the presence of the pentasaccharide. The change in mobility consequent to deimination occurs only in lane 6, with the P_1 Arg antithrombin plus pentasaccharide.

The pentasaccharide used in this study was obtained in the framework of a Sanofi–Organon (C. van Boeckel) collaboration on antithrombotic oligosaccharides. This work was supported by the Wellcome Trust, the Medical Research Council of Great Britain, and the British Heart Foundation. L.J. has a Wellcome Prize Studentship and support from the Sackler and Cambridge Commonwealth funds.

1. Marcum, J. A., McKenney, J. B., Galli, S. J., Jackman, R. W. & Rosenberg, R. D. (1986) *J. Clin. Invest.* **74,** 341–350.
2. Thunberg, L., Backstrom, G. & Lindahl, U. (1982) *Carbohydr. Res.* **100,** 393–397.
3. Choay, J., Petitou, M., Lormeau, J. C., Sinay, P., Casu, B. & Gatti, G. (1983) *Biochem. Biophys. Res. Commun.* **116,** 492–499.
4. Lane, D. A., Denton, J., Flynn, A. M., Thunberg, L. & Lindahl, U. (1984) *Biochem. J.* **218,** 725–732.
5. Olson, S. T., Björk, I., Sheffer, R., Craig, P. A., Shore, J. D. & Choay, J. (1992) *J. Biol. Chem.* **267,** 12528–12538.
6. Carrell, R. W., Evans, D. L. & Stein, P. E. (1991) *Nature (London)* **353,** 576–578.
7. Gettins, P. G., Fan, B., Crews, B. C., Turko, I. V., Olson, S. T. & Streusand, V. J. (1993) *Biochemistry* **32,** 8385–8389.
8. Carrell, R., Skinner, R., Wardell, M. & Whisstock, J. (1995) *Mol. Med. Today* **1,** 226–231.
9. Huber, R. & Carrell, R. W. (1989) *Biochemistry* **28,** 8951–8966.
10. Loebermann, H., Tokuoka, R., Deisenhofer, J. & Huber, R. (1984) *J. Mol. Biol.* **177,** 531–556.
11. Wright, H. T. & Scarsdale, J. N. (1995) *Proteins* **22,** 210–225.
12. Björk, I., Nordling, K. & Olson, S. T. (1993) *Biochemistry* **32,** 6501–6505.
13. Schreuder, H. A., de Boer, B., Dijkema, R., Mulders, J., Theunissen, H. J. M., Grootenhuis, P. D. J. & Hol, W. G. J. (1994) *Nat. Struct. Biol.* **1,** 48–54.
14. Carrell, R. W., Stein, P. E., Fermi, G. & Wardell, M. R. (1994) *Structure* **2,** 257–270.
15. Skinner, R., Abrahams, J. P., Whisstock, J. C., Lesk, A. M., Carrell, R. W. & Wardell, M. R. (1997) *J. Mol. Biol.* **266,** 601–609.
16. Van Boeckel, C. A. A. & Petitou, M. (1993) *Angew. Chem.* **32,** 1671–1818.
17. Basten, J., Jaurand, G., Olde-Hanter, B., Duchaussoy, P., Petitou, M. & van Boeckel, C. A. A. (1992) *BioMed. Chem. Lett.* **2,** 905–910.
18. Leslie, A. W. G. (1992) *Recent Changes to the MOSFLM Package for Processing Film and Image Data* (Daresbury Laboratory, Warrington, U.K.).
19. Collaborative, C. P. N.4. (1994) *Acta Crystallogr. D* **50,** 760–763.
20. Navaza, J. (1994) *Acta Crystallogr. A* **50,** 157–163.
21. Brünger, A. T. (1993) XPLOR Manual (Yale University), Version 3.1.
22. Abrahams, J. P. (1996) *Likelihood-Weighted Real Space Restraints for Refinement at Low Resolution* (Daresbury Laboratory, Warrington, U.K.).
23. Tronrud, D. E., Ten Eyck, L. F. & Matthews, B. W. (1992) *Acta Crystallogr. A* **43,** 489–501.
24. Laskowski, R. A., MacArthur, M. W., Moss, D. S. & Thornton, J. M. (1994) *J. Appl. Crystallogr.* **26,** 283–291.
25. Kraulis, P. (1991) *J. Appl. Crystallogr.* **24,** 946–950.
26. Owen, M. C., Beresford, C. H. & Carrell, R. W. (1988) *FEBS Lett.* **231,** 317–320.

27. Borg, J.-Y., Owen, M. C., Soria, J., Caen, J. & Carrell, R. W. (1988) *J. Clin. Invest.* **81,** 1292–1296.
28. Kridel, S. J., Chan, W. W. & Knauer, D. J. (1996) *J. Biol. Chem.* **271,** 20935–20941.
29. Van Boeckel, C. A. A., Grootenhuis, P. D. J. & Visser, A. (1994) *Nat. Struct. Biol.* **1,** 423–425.
30. Mourey, L., Samama, J.-P., Delarue, M., Petitou, M., Choay, J. & Moras, D. (1993) *J. Mol. Biol.* **232,** 223–241.
31. Jordan, R. E., Nelson, R. M., Kilpatrick, J., Newgren, J. O., Esmon, P. C. & Fournel, M. A. (1989) *J. Biol. Chem.* **264,** 10493–10500.
32. Elliott, P. R., Lomas, D. A., Carrell, R. W. & Abrahams, J. P. (1996) *Nat. Struct. Biol.* **3,** 676–681.
33. Pike, R. N., Potempa, J., Skinner, R., Fitton, H. L., McGraw, W. T., Travis, J., Owen, M., Jin, L. & Carrell, R. W. (1997) *J. Biol. Chem.* **272,** 19652–19655.
34. Takahara, H., Okamoto, H. & Sugawara, K. (1985) *J. Biol. Chem.* **260,** 8378–8383.
35. Meagher, J. L., Huntington, J. A., Fan, B. & Gettins, P. G. W. (1996) *J. Biol. Chem.* **271,** 29353–29358.
36. Huntington, J. A., Olson, S. T., Fan, B. & Gettins, P. G. W. (1996) *Biochemistry* **35,** 8495–8503.
37. Kappers-Klunne, M. C., Boon, D. M. S., Hop, W. C. J., Michiels, J. J., Stibbe, J., van der Zwaan, C., Koudstaal, P. J. & van Vliet, H. H. D. M. (1997) *Br. J. Haematol.* **96,** 442–446.
38. Lander, A. D. (1994) *Chem. Biol.* **1,** 73–78